Osthole Inhibits Osteoclast Formation and Enhances Bone Mass of Bone Marrow Mesenchymal Stem cells by Activating β-catenin-OPG Signaling Pathway

Zhen-Xiong Jin
Longhua hospital
Xin-Yuan Liao
spine center
Wei-Wei Da
longhua hospital
Yong-Jian Zhao
shanghai university of traditional chinese medicine
Xiao-Feng Li
Shanghai University of Traditional Chinese Medicine
Dezhi Tang (dzt702@163.com)
longhua hospital

Research

Keywords: Osthole, β-catenin, Osteoprotegerin, Osteoclast, Osteoporosis

Posted Date: December 28th, 2020

DOI: https://doi.org/10.21203/rs.3.rs-133397/v1

Version of Record: A version of this preprint was published on February 27th, 2021. See the published version at https://doi.org/10.1186/s13287-021-02228-6.

Abstract

Summary Osthole has potential therapeutic applications due to its antiosteoporotic. Our study suggested that osthole attenuates osteoclast formation by stimulating the activation of β-catenin-OPG signaling and could be a potential agent to inhibit bone resorption.

Introduction Osthole has potential therapeutic applications due to its antiosteoporotic. we performed study to test if OPG is the target gene of osthole-attenuated osteoclastogenesis.

Methods In vivo, using 12-month-old male mice to evaluate the effect of osthole on bone mass. In vitro, Bone marrow stem cells (BMSCs) were isolated, extracted from 3-month-old C57BL/6J mice, 3-month-old β-catenin$^{fx/fx}$ mice, or 3-month-old OPG$^{-/-}$ mice and its littermates of OPG$^{+/+}$ mice.

Results we found that osthole significantly increased the gene and protein levels of OPG expression in primary BMSCs dose-dependently. The deletion of the OPG gene did not affect β-catenin expression and the deletion of the β-catenin gene inhibited OPG expression in BMSCs, which indicated that osthole stimulated the expression of OPG through activation of β-catenin signaling.

Conclusion Osthole attenuates osteoclast formation by stimulating the activation of β-catenin-OPG signaling and could be a potential agent to inhibit bone resorption.

Introduction

Osteoporosis is a systematic skeletal disease that thins and weakens the bones to the point that they become fragile and break easily, is one of the most disabling consequences of aging[1–2]. Hip fractures and vertebral fractures are strongly associated with reductions in BMD, and have been considered the prototypical osteoporotic fractures[3]. In 2010, an estimated 2.7 million hip fractures occurred worldwide, and half of them (51%) were considered preventable[4–5]. However, the incidence of all other fractures (non-hip, non-vertebral) is numerically much greater and collectively these fractures result in much larger economic costs for the population[6]. Fractures show symptoms of pain and an inability to bear weight, almost always require surgical fixation[7]. In addition, the patient's functional status and quality of life are reduced, with a high risk for short-term mortality, as well as a lot of direct medical expenses[8–9].

Estrogen replacement therapy are effective in increasing osteoblast activity, but resulted in the increased incidence of breast and uterine cancer[10–11]. Phytoestrogens have attracted attention to their potential impacts in the prevention and treatment for osteoporosis. Osthole, a coumarin derivative extracted from Cnidiummonnieri and Angelica of Chinese herbal medicine, has estrogenic effect in preventingagainst bone loss in ovariectomizedrat[12–13]. Numerous studies have confirmed a wide range of pharmacological activities of osthole in humans, such as anti-cancer activity, antihypertensive, anti-arrhythmic, anti-inflammatory, anti-infection properties and promote osteoblasts differentiation[14–16].

Bone marrow stem cells (BMSCs) have differentiation into osteogenic, fat, cartilage and nerve-like cells, and it have strong in vitro expansion capacity, as well as the potential for multi-directional differentiation[17–18]. Recent technological advances in cell labeling and tracing have facilitated the study of underlying mechanisms[19–20]. Used lineage tracing methods and proposed that bone marrow cells expressing Mx1 have all the known characteristics of BMSCs. These cells respond to tissue stress and migrate to sites of injury, supplying new osteoblasts during fracture healing[21]. In addition, Leptin Receptor (LepR) is another marker for identifying BMSC. LepR positive cells have been shown to produce osteoblasts and adipocytes in bone marrow[22]. Besides, cells expressing gremlin-1 have been isolated from bone marrow, and these cells are capable of bone formation, rather than adipogenesis[23]. This also makes BMSCs widely used in clinical research at the cellular level of bone and cartilage tissues, including cartilage repair.

Our previous study found that Osthole significantly stimulated osteoblast differentiation and bone formation by inducing the activation of Wnt/β-catenin-Bmp2 signaling[24]. And our previous meta-analysis of basic reports shows that BMSCs can promote bone call maturation, ossification and restore bone mechanical properties in osteoporotic fractures[25]. Although Osthole can promote bone formation, its effect on bone resorption and underlying mechanism remain unknown. In this study, we performed the in vivo and in vitro experiments to examine the effect of Ostholeon osteoclast formation.

Materials And Methods

Mice and reagents

All animal protocols were approved by Institutional Review Board of Longhua hospital, Shanghai University of Traditional Chinese Medicine (China). C57BL/6J wild-type mice, OPG knockout (KO) mice and OPG Wild-type (WT) mice were purchased from Shanghai Biomodel Organism Science & Technology Development Co.,Ltd(China). Osthole, with 98% purity, was purchased from the Shanghai Institute for Drug and Quarantine Bureau. Recombinant human M-CSF and the receptor activator of nuclear factor-kappa B ligand (RANKL) proteins were purchase from R&D system (Minneapolis, MN, USA). Dimethyl sulfoxide (DMSO) was purchased from Sigma-Aldrich (St. Louis, MO, USA). Fetal bovine serum, DMEM dehydrated medium, and penicillin streptomycin combination were purchased from Invitrogen Corporation (Carlsbad, CA). RNeasy Mini RNA kit was purchased from Qiagen Corporation (Valencia, CA). iScriptcDNA synthesis kit and PVDF membrane were purchased from Bio-Rad Laboratories, Inc (Hercules, CA). Absolute QPCR SYBR Green Master Mix and E-PER protein extraction reagents were purchased from Thermo Scientific (Waltham, MA). Tartrate-resistant acid phosphatase staining (Trap) kit was purchased from Sigma-Aldrich (St. Louis, MO). Mouse bone gla-protein (BGP) ELISA kit was purchased from GENTAUR (SanJose, CA). Rabbit anti-OPG monoclonal antibody, Rabbit anti-*β*-catenin monoclonal antibody and mouse anti-β-Actin monoclonal antibody were purchased from Cell Signaling Technology, Inc (Beverly, MA). Adenovirus-GFP and Adenovirus -Cre were purchased from Baylor College of Medicine (Houston, TX, USA).

Animal study

Twelve12-month-old male mice were randomized into two groups, treatment group and control group, respectively. The treatment group was intervened with Osthole (5 mg/kg/day) by intraperitoneal injection once a day for 4 weeks, and the control group was intervened with vehicle (corn oil) by intraperitoneal injection once a day for 4 weeks. After sacrificed, the lumbar vertebrae were harvested for evaluation.

Micro-computed tomography (μCT) analysis

The fifth lumbar vertebrae (L5) were scanned at 18-μm voxel size using the μCT scanner (μCT80, Scanco Medical AG, Bassersdorf, Switzerland). The trabecular bone under the growth plate was segmented using a contouring tool, and the contours were morphed automatically to segment the trabecular bone on all the one-hundred slices. The 3D images were reconstructed and analyzed with the evaluation software of the μCT system.

Histological and histomorphometrical assays

The third lumbar vertebrae (L3) were fixed in 4% paraformaldehyde, decalcified, dehydrated, cleared with dimethylbenzene, and then embedded in paraffin. At least 3 consecutive 7-μm sectionswere obtained from the coronal planes, and performed TRAPstaining for identifying osteoclasts. Histomorphometrical assay was performed to determine the number of osteoclasts andthe percentage of osteoclast surface by using an imageauto-analysis system (Olympus BX50; Japan).

Immunohistochemical staining

The paraffin sections of L3were deparaffinized by immersing the tissue in xylene, fixing it with4% paraformaldehyde for 15 minutes, and treating it with0.5% Triton for 15 minutes, followed by fixation with 4%paraformaldehyde for another 5 minutes.The sections were then incubated with rabbit anti-OPG monoclonal antibody(1:50dilution) and rabbit anti-β-catenin monoclonal antibody(1:50dilution), at 4 °C over night. Afterthorough wash, the slides were then incubated with a horseradish peroxidase (HRP)–conjugated secondary antibody for 30 minutes. After being mounted, slides wereexamined by using an Image Analysis System (OlympusBX50, Japan).

Bone marrow stemcells (BMSCs) culture and treatment

Primary bone marrow stem cells, extracted from 3-month-old C57BL/6J mice, or 3-month-old $OPG^{-/-}$ mice and its littermates of $OPG^{+/+}$ mice, were cultured with incubation of M-CSF and RANKL for one week, and then treated with various doses (0.5-100 μM) of Osthole for 48 hours.

TRAP staining

Primary BMCswere seeded in 96-well plate at a density of $3x10^5$/ml. The cells were treated with M-CSF (30 ng/ml) and RANKL (30 ng/ml), at the present or absence of Osthole (100 μM).The medium was

changed every 3 days. After 7-day-incubation, the cells was fixed and performed TRAP staining to calculate the number of multi-nuclear (>=3 nucleus) osteoclasts.

Real-time qPCR analysis

Primary BMSCs extracted from 3-month-old C57BL/6J mices, were seeded in 6-well plates at a density of $1x10^6$ cells/well. After 2-day culture, Cells were treated with variation doses of Osthole (1-100 μM) or Vehicle for 48 hours. Total cellular mRNA was isolated respectively using RNeasy Mini Kit. One microgram of total RNA was reverse-transcribed separately into cDNA using the iScriptcDNA synthesis kit. Quantitative polymerase chain reaction (qPCR) analysis was carried out using Absolute QPCR SYBR Green Master Mix in a total volume of 20 μl of buffered solution containing 1μl of the diluted (1:5) reverse transcription product in the presence of sense and antisense primers of target genes listed as Table 1. *β*-actin is internal reference gene. Conditions were 15-min polymerase activation at 95 °C followed by 45 cycles, 95 °C for 20 s, 58 °C for 20 s and 72 °C for 30 s. All reactions were performed in triplicate independently.

Western-blotting analysis

Primary BMSCs isolated from 3-month-old $OPG^{-/-}$ homozygous mice and its littermates of $OPG^{+/+}$ mice, were seeded in 6-well plates at a density of $1x10^6$ cells/well. Cells were treated with Osthole (100 μM) or Vehicle for 48 hours and cells lysates were, respectively, extracted with E-PER protein extraction reagents (Thermo Scientific, Waltham, MA). Proteins were transferred onto a PVDF membrane (Bio-Rad, Hercules, CA) and the membrane was blocked with 5% non-fat milk in PBST solution for 1 h at room temperature (RT). After incubation with the primary antibody overnight at 4 °C and the HRP-conjugated secondary antibodies (Thermo Scientific, Waltham, MA) for 1 h at RT, the protein expression was detected using a SuperSignal West Femto Maximum Sensitivity Substrate Kit (Thermo Scientific, Waltham, MA). Rat anti-OPG monoclonal antibody and Rabbit anti-*β*-catenin monoclonal antibody were used as primary antibodies. Mouse anti-*β*-Actin monoclonal antibody was used as secondary antibody.

In vitro deletion of the *β*-catenin gene

In vitro deletion of the *β*-catenin gene was performed as previouslydescribed[24]. BMSCs isolated from 3-month-old *β*-$catenin^{fx/fx}$ mice were seeded in 6-well culture plates at a density of 1×10^6 cells per well and cultured for6 days. Cells were infected with Ad-GFP or Ad-Cre (Titer:4×10^8 pfu/mL; Baylor College of Medicine, Houston, TX,USA) for 72 hours. Ad-GFP was used as a control and tomonitor infection efficiency. After recovery for 48 hours, cellswere treated with or without Osthole (100 uM) for 48 hours. Real-time qPCR assay was performed to examine the expression of *β*-catenin and OPG. All reactions were performed in triplicate independently.

Statistical analysis

Based on all experiments conducted independently at least three times, the date was expressed as mean ± SD and analyzed using SPSS 24.0 software and GraphPad Prism 8. We analyzed the statistically significant differences using Student's t test and one-way analysis of variance. ImageJ software was employed to measure the grayscale analyses. In figures,*$P < 0.05$ or lower was considered statistically significant.

Results

Bone loss was reduced in twelve-month-old mice

Three-month-old and twelve-month-old C57BL/6J mice were used to evaluate bone mass. The μCT 3D image analysis on the forth lumbar vertebrae (L4) showed the loss of trabecular bone of twelve-month-old mice compared with that of three-month-old mice (Fig. 1A). The quantitative analysis showed that bone volume over total volume (BV/TV) and bone mineral density (BMD) of aged mice were significantly decreased ($p < 0.05$, Fig. 1B, 1C) as compared to those of young mice,suggesting that the aged mice displayed decreased bone mass.

Osthole Inhibited Aging-induced Bone Loss

Osthole significantly increased bone mass of aged mice (Fig. 2A). The quantitative analysisshowed an apparent increase in ($p < 0.05$) 67% of BMD ($p < 0.05$)and 75% of BV/TV in aged mice after treated with Osthole(Fig. 2B, C). And Osthole was found to significantly increase Tb.N($p < 0.05$, Fig. 2D)and decrease Tb.Sp($p < 0.05$, Fig. 2E).These data demonstrated that Osthole inhibited ageing-induced bone loss.

Osthole Inhibited Osteoclast Formation In Aged Mice

TRAP stainingwas performedon sections of L5. Osthole decreased the TRAP-positive number of multinucleated osteoclast (Fig S1A, B), moreover, redcued the percentage of osteoclast surface in aged mice after treated with Osthole (Figure S1C).These data showed that Osthole could inhibit osteoclast formation in aged mice. However, we found that Osthole could not inhibit osteoclast formation in OPG gene knockout mice (Figure S1D,E), suggesting that effect of Osthole may be through the OPG signaling.

Osthole inhibited osteoclastogenesis in a dose-dependent and an OPG-dependent manner

OPG/RANKL signaling has been shown to play an important role in osteoclast formation. To determine the mechanism of Osthole on suppressing osteoclast formation, we examined the effect of Osthole on the expression of OPG and RANKL. Osthole(10, 50, 100 μM) also significantly enhanced OPG mRNA expressionin a dose-dependent manner ($P < 0.05$) and Osthole at the dose of 100 μM had the maximum effect with 3.8-fold increase (Fig. 3A). In contrast, Osthole had no effect on the expression of RANKL

(data not shown). We also examined the effect of Osthole on protein expression of OPG and found that Osthole significantly increased the protein level of OPG mRNA in a dose-dependent manner (Fig. 3B)

To further determine if Osthole-inhibited-osteoclastogenesis is OPG dependent, BMCs were isolated from 3-month-old $OPG^{-/-}$ mice and its littermates of $OPG^{+/+}$ mice, cultured with M-CSF (44 ng/ml) and RANKL (100 ng/ml), plus Osthole (100 μM) or vehicle for 7 days, then TRAP staining were performed and osteoclast number was quantificated. As shown in Fig. 3C and 3D, Osthole significantly inhibited osteoclast formation in $OPG^{+/+}$ mice($P < 0.05$), in contrast, in $OPG^{-/-}$ mice it had no effect on the formation of osteoclast. These data suggested that Osthole inhibits osteoclastogenesis in an OPG-dependent manner.

Osthole promoted the expression of OPG through activation of β-catenin signaling

Our recent studies have demonstrated that OPG expression could be activated by β-catenin signaling and Osthole could activate *β*-catenin signaling [24, 26–27]. We first examined OPG and *β*-catenin expression in vivo. The immunostaining data showed that Osthole significantly increased OPG protein level (Fig. 4A) and *β*-catenin protein level (Fig. 4B) using sections of L5 samples in aged mice. To further confirm if Osthole-induced-OPG expression is through *β*-catenin signaling, we performed in vitro study. Primary BMSCs were isolated from 3-month-old *β*-$Catenin^{fx/fx}$ mice, infected with Ad-Cre or Ad-GFP, and treated with or without Osthole at the dose of 100uM. After 2 days, the total mRNA was collected and the expression of OPG was detected using real-time PCR assay. We found that the deletion of *β*-Catenin by Ad-Cre infection significantly inhibited Osthole-induced expression of OPG (Fig. 4C). In contrast, we found that the deletion of OPG didn't affect Osthole-induced expression of *β*-Catenin protein (Fig. 4D). Taken together, these results indicated that Osthole promotes the expression of OPG through activation of *β*-catenin signaling.

Discussion

The present study discovered that Osthole inhibited bone resorption in aged mice and attenuated osteoclast formation through stimulatingthe activation of *β*-catenin-OPG signaling (Fig. 5). Osteoporosis is caused by the disorder of homeostasis between bone formation and bone resorption. Our previous results showed that Osthole has an efficacy to promote osteoblastic proliferation and differentiation as well as act on the bone metabolism[24]. Whether Osthole impacts on the function of osteoclasts is the aim of this study. Osthole was firstly used to intervene with the elderly wild-type mice. The μCT analysis showed that the treatment with Osthole for 4 weeks could significantly increase bone mass in senile mice. One of the important reasons for the occurrence of osteoporosis is the increased activity and quantity of osteoclasts. Thus, TRAP staining was performed and the results demonstrated that the number of osteoclasts obviously was decreased in senile mice after intraperitoneal injection with Osthole. In order to further confirm this effect, the dose-dependent effect of Osthole on osteoclasts,derived from primary BMSCs upon to M-CSF and RANKL, was studied. Our results showed that Osthole could obviously decrease the number of osteoclasts in a dose-dependent manner. We also performed pits

assay on bone slices and found that Osthole could attenuate the activity of functional osteoclasts. Together, Osthole could inhibit osteoclast formation and osteoclast-involved bone resorptive activity.

We further investigated the mechanism of Osthole on osteoclast formation. Under normal physiological conditions, the resorption of cartilage and bone is essential for development and regeneration of skeleton[28]. Osteoclastogenesis is a complicated process regulated by finely orchestrated interactions between osteoclast precursors and osteoblasts/stromal cells in bone marrow environment[29–30].Osteoblasts produce OPG, which is a decoy receptor for the receptor activator of RANKL. By binding RANKL, OPG inhibits the interaction between RANKL and the receptor activator of nuclear factor-kappa B (RANK), a receptor of RANKL, therefore, OPG/RANKL/RANK plays key roles in the process of osteoclastogenesis[31–32]. Our data showed that Osthole significantly promoted the expression of OPG in BMSCs with a dose-dependent manner, but did notshow obvious effect on RANKL expression. RANKL is generally essential for osteoclast formation and thought to be supplied by osteoblasts or their precursors[33]. In contrast, recent evidences have revealed that osteocytes express high levels of RANKL and contribute to the coupling of bone formation and bone resorption[34–35].Here we found that Osthole did not have any effect on RANKL expression in BMSCs, indicating that it may generate the effect on the expression of RANKL in osteocytes.

To demonstrate if Osthole-inhibited osteoclastogenesis was OPG-dependent, we next performed a rescue experiment using BMSCs from $OPG^{+/+}$ and $OPG^{-/-}$ mice. Osthole decreased the formation of osteoclastsin $OPG^{+/+}$ mice, while it had no effect in $OPG^{-/-}$ mice. Therefore, our result indicated that Osthole-attenuated osteoclastogenesis was through increasing the expression of OPG in BMSCs and inhibiting the binding of RANKL and RANK, but not acting on RANKL and RANK directly. The underlying mechanism of Osthole on the regulation of OPG was further studied for OPG upstream signaling. It has been reported that the canonical Wnt pathway up-regulates the expression of OPG in osteoblasts and chondrocytes[36–37]. β-catenin, a key protein of the canonical Wnt pathway, is required to induce the expression of OPG in osteoblasts[38]. In addition, it is reported that polydatin improved the osteogenic differentiation of hBMSCs and maintained the bone matrix in the OVX mouse model through the activation of β-catenin pathway[39]. Melatonin promotes the BMP9-induced osteogenic differentiation of mesenchymal stem cells by activating the β-catenin signalling pathway[40]. But inactivation of β-catenin signaling in osteoblasts causedthe increased osteoclastogenesis due to insufficient production of OPG[41]. Wnt3a was unable to induce the production of normal OPG to inhibit bone resorption, while lacking of β-catenin in osteoclasticlineage[36, 41]. Cellular and molecular studies have shown that β-catenin banding with TCF proteins regulates the expression of OPG in osteoblasts[42]. Here we found Osthole could significantly increase the expression of β-catenin and OPG in BMSCs. To further discuss the interactions between β-catenin and OPG, we performed the rescue experiment in vitro using β-catenin floxed mice and found that the deletion of the β-catenin gene could inhibit Osthole-induced OPG expression. This result demonstrated that Osthole stimulated the expression of OPG through the β-catenin signaling.

Canonical Wnt signaling is required for the differentiation of mesenchymal progenitors into osteoblasts, as well as importance to the connection between osteoblasts and bone metabolism[43–44]. Wnt3a is an important upstream gene to regulate this pathway. The proteins complex of Wnt3a, Frizzled8 and LRP5/6 inhibits the activity of GSK3β, which makes β-catenin to be phosphorylated and degraded.Then β-catenin is released and translocated to the nucleus, where it interacts with TCF/LEF transcription factors to activate the expression of target genes. Released β-catenin may also interact with site2 and site4 on the OPG promoter directly, to increase production and secretion of OPG and inhibit the binding of RANKL and RANK, thus reduces the formation and activity of osteoclast[42]. It has been reported that BMP2 can also increase the expression of OPG by up-regulating Wnt3aexpression and promoting Samd1/4 to interact with site2 and site4 on OPG promoter[45]. In contrast, Wnt5a activates the non canonical Wnt signaling, which increases the activity of RANKL to promote osteoclastogenesis[47]. Our previous study showed that Osthole could significantly stimulate the expression of Wnt3a, but not Wnt5a[24].

Conclusion

Based on the above discussions, we concluded that Osthole inhibited osteoclast formation and bone resorption through stimulating the activation of Wnt3a/β-catenin-OPG signaling (Fig. 6).

Abbreviations

OPG: osteoprotegerin; μCT: micro-computed tomography; BMSCs: Bone marrow stem cells; LepR: Leptin Receptor; KO: knockout; WT: Wild-type; DMSO: Dimethyl sulfoxide; BGP: bone gla-protein; qPCR: Quantitative polymerase chain reaction; RT: room temperature; RANK: receptor activator of nuclear factor-kappa B; RANKL: the receptor activator of nuclear factor-kappa B ligand.

Declarations

Acknowledgements

We thank the team for their cooperation.

Authors' contributions

Conceived and designed the experiments: De-Zhi Tang

Performed the experiments: Zhen-Xiong Jin and Xin-Yuan Liao

Analyzed the data: Zhen-Xiong Jin, Xin-Yuan Liao and Wei-Wei Da

Contributed funders/reagents/materials/analysis tools: Yong-Jian Zhao and Xiao-Feng Li

The authors read and approved the final manuscript.

Funding

This work was sponsored by the National Natural Science Foundation (81973883) and Shanghai Natural Science Foundation (19ZR1458000).

Availability of data and materials

The datasets used and/or analyzed during the current study are available from the corresponding author on reasonable request.

Ethics approval and consent to participate

This research has been approved by the Ethics Committee of Longhua Hospital Affiliated to Shanghai University of Traditional Chinese Medicine.

Compliance with ethical standards

Conflicts of interest Zhen-Xiong Jin, Xin-Yuan Liao, Wei-Wei Da, Yong-Jian Zhao, Xiao-Feng Li and De-Zhi Tang declare that they have no conflict of interest.

Consent for publication

All authors have agreed to publish.

References

1. Black DM, Geiger EJ, Eastell R, Vittinghoff E, Li BH, Ryan DS, Dell RM, Adams AL. Atypical Femur Fracture Risk versus Fragility Fracture Prevention with Bisphosphonates. N Engl J Med. 2020;383(8):743–53.
2. Estell EG, Rosen CJ. Emerging insights into the comparative effectiveness of anabolic therapies for osteoporosis. NAT REV ENDOCRINOL 2020.
3. Compston JE, McClung MR, Leslie WD. Osteoporosis. LANCET. 2019;393(10169):364–76.
4. Oden A, McCloskey EV, Johansson H, Kanis JA. Assessing the impact of osteoporosis on the burden of hip fractures. Calcif Tissue Int. 2013;92(1):42–9.
5. Unim B, Minelli G, Da CR, Manno V, Trotta F, Palmieri L, Galluzzo L, Maggi S, Onder G. Trends in hip and distal femoral fracture rates in Italy from 2007 to 2017. BONE 2020: 115752.
6. Leslie WD, Metge CJ, Azimaee M, Lix LM, Finlayson GS, Morin SN, Caetano P. Direct costs of fractures in Canada and trends 1996–2006: a population-based cost-of-illness analysis. J BONE MINER RES. 2011;26(10):2419–29.
7. Laine JC, Novotny SA, Weber EW, Georgiadis AG, Dahl MT. Distal Tibial Guided Growth for Anterolateral Bowing of the Tibia: Fracture May Be Prevented. J BONE JOINT SURG AM 2020.

8. Khosla S, Hofbauer LC. Osteoporosis treatment: recent developments and ongoing challenges. Lancet Diabetes Endocrinol. 2017;5(11):898–907.
9. Morgan EF, Unnikrisnan GU, Hussein AI. Bone Mechanical Properties in Healthy and Diseased States. ANNU REV BIOMED ENG. 2018;20:119–43.
10. Li B, Liu M, Wang Y, Gong S, Yao W, Li W, Gao H, Wei M. Puerarin improves the bone micro-environment to inhibit OVX-induced osteoporosis via modulating SCFAs released by the gut microbiota and repairing intestinal mucosal integrity. BIOMED PHARMACOTHER. 2020;132:110923.
11. Compston JE. Sex steroids and bone. PHYSIOL REV. 2001;81(1):419–47.
12. Yun C, Wu S, Xin-xin Z, Yan-die L, Hao C, Hao LI. Osthole prevents acetaminophen-induced liver injury in mice. Acta Pharmacol Sin. 2018;39(1):74–84.
13. Zhang Z, Leung W, Li G, Kong S, Lu X, Wong Y, Chan C. Osthole Enhances Osteogenesis in Osteoblasts by Elevating Transcription Factor Osterix via cAMP/CREB Signaling In Vitro and In Vivo. NUTRIENTS 2017, **9**(6): 588.
14. Dai X, Yin C, Zhang Y, Guo G, Zhao C, Wang O, Xiang Y, Zhang X, Liang G. Osthole inhibits triple negative breast cancer cells by suppressing STAT3. J EXP CLIN CANC RES 2018, 37(1).
15. Hassanein E, Sayed AM, Hussein OE, Mahmoud AM. Coumarins as Modulators of the Keap1/Nrf2/ARE Signaling Pathway. OXID MED CELL LONGEV 2020, **2020**: 1675957.
16. Gao LN, An Y, Lei M, Li B, Yang H, Lu H, Chen FM, Jin Y. The effect of the coumarin-like derivative osthole on the osteogenic properties of human periodontal ligament and jaw bone marrow mesenchymal stem cell sheets. BIOMATERIALS. 2013;34(38):9937–51.
17. Ma Y, Ran D, Cao Y, Zhao H, Song R, Zou H, Gu J, Yuan Y, Bian J, Zhu J, Liu Z. The effect of P2 × 7 on cadmium-induced osteoporosis in mice. J HAZARD MATER 2020: 124251.
18. Kfoury Y, Scadden DT. Mesenchymal cell contributions to the stem cell niche. CELL STEM CELL. 2015;16(3):239–53.
19. Xu R, Yallowitz A, Qin A, Wu Z, Shin DY, Kim JM, Debnath S, Ji G, Bostrom MP, Yang X, Zhang C, Dong H, Kermani P, Lalani S, Li N, Liu Y, Poulos MG, Wach A, Zhang Y, Inoue K, Di Lorenzo A, Zhao B, Butler JM, Shim JH, Glimcher LH, Greenblatt MB. Targeting skeletal endothelium to ameliorate bone loss. NAT MED. 2018;24(6):823–33.
20. Curtis M, Kenny HA, Ashcroft B, Mukherjee A, Johnson A, Zhang Y, Helou Y, Batlle R, Liu X, Gutierrez N, Gao X, Yamada SD, Lastra R, Montag A, Ahsan N, Locasale JW, Salomon AR, Nebreda AR, Lengyel E. Fibroblasts Mobilize Tumor Cell Glycogen to Promote Proliferation and Metastasis. CELL METAB. 2019;29(1):141–55.
21. Park D, Spencer JA, Koh BI, Kobayashi T, Fujisaki J, Clemens TL, Lin CP, Kronenberg HM, Scadden DT. Endogenous bone marrow MSCs are dynamic, fate-restricted participants in bone maintenance and regeneration. CELL STEM CELL. 2012;10(3):259–72.
22. Zhou BO, Yue R, Murphy MM, Peyer JG, Morrison SJ. Leptin-receptor-expressing mesenchymal stromal cells represent the main source of bone formed by adult bone marrow. CELL STEM CELL. 2014;15(2):154–68.

23. Worthley DL, Churchill M, Compton JT, Tailor Y, Rao M, Si Y, Levin D, Schwartz MG, Uygur A, Hayakawa Y, Gross S, Renz BW, Setlik W, Martinez AN, Chen X, Nizami S, Lee HG, Kang HP, Caldwell JM, Asfaha S, Westphalen CB, Graham T, Jin G, Nagar K, Wang H, Kheirbek MA, Kolhe A, Carpenter J, Glaire M, Nair A, Renders S, Manieri N, Muthupalani S, Fox JG, Reichert M, Giraud AS, Schwabe RF, Pradere JP, Walton K, Prakash A, Gumucio D, Rustgi AK, Stappenbeck TS, Friedman RA, Gershon MD, Sims P, Grikscheit T, Lee FY, Karsenty G, Mukherjee S, Wang TC. Gremlin 1 identifies a skeletal stem cell with bone, cartilage, and reticular stromal potential. CELL. 2015;160(1–2):269–84.
24. Tang DZ, Hou W, Zhou Q, Zhang M, Holz J, Sheu TJ, Li TF, Cheng SD, Shi Q, Harris SE, Chen D, Wang YJ. Osthole stimulates osteoblast differentiation and bone formation by activation of beta-catenin-BMP signaling. J BONE MINER RES. 2010;25(6):1234–45.
25. Jin Z, Chen J, Shu B, Xiao Y, Tang D. Bone mesenchymal stem cell therapy for ovariectomized osteoporotic rats: a systematic review and meta-analysis. BMC Musculoskelet Disord. 2019;20(1):556.
26. Yan Y, Tang D, Chen M, Huang J, Xie R, Jonason JH, Tan X, Hou W, Reynolds D, Hsu W, Harris SE, Puzas JE, Awad H, O'Keefe RJ, Boyce BF, Chen D. Axin2 controls bone remodeling through the beta-catenin-BMP signaling pathway in adult mice. J CELL SCI. 2009;122(Pt 19):3566–78.
27. Zhu M, Tang D, Wu Q, Hao S, Chen M, Xie C, Rosier RN, O'Keefe RJ, Zuscik M, Chen D. Activation of beta-catenin signaling in articular chondrocytes leads to osteoarthritis-like phenotype in adult beta-catenin conditional activation mice. J BONE MINER RES. 2009;24(1):12–21.
28. Tsukasaki M, Takayanagi H. Osteoimmunology: evolving concepts in bone-immune interactions in health and disease. NAT REV IMMUNOL. 2019;19(10):626–42.
29. Shin CS, Her SJ, Kim JA, Kim DH, Kim SW, Kim SY, Kim HS, Park KH, Kim JG, Kitazawa R, Cheng SL, Civitelli R. Dominant negative N-cadherin inhibits osteoclast differentiation by interfering with beta-catenin regulation of RANKL, independent of cell-cell adhesion. J BONE MINER RES. 2005;20(12):2200–12.
30. Charles JF, Aliprantis AO. Osteoclasts: more than 'bone eaters'. TRENDS MOL MED. 2014;20(8):449–59.
31. Lacey DL, Boyle WJ, Simonet WS, Kostenuik PJ, Dougall WC, Sullivan JK, San MJ, Dansey R. Bench to bedside: elucidation of the OPG-RANK-RANKL pathway and the development of denosumab. NAT REV DRUG DISCOV. 2012;11(5):401–19.
32. Feng X, McDonald JM. Disorders of bone remodeling. Annu Rev Pathol. 2011;6:121–45.
33. Lv WT, Du DH, Gao RJ, Yu CW, Jia Y, Jia ZF, Wang CJ. Regulation of Hedgehog signaling Offers A Novel Perspective for Bone Homeostasis Disorder Treatment. INT J MOL SCI 2019, 20(16).
34. Davaine JM, Quillard T, Chatelais M, Guilbaud F, Brion R, Guyomarch B, Brennan MA, Heymann D, Heymann MF, Goueffic Y. Bone Like Arterial Calcification in Femoral Atherosclerotic Lesions: Prevalence and Role of Osteoprotegerin and Pericytes. Eur J Vasc Endovasc Surg. 2016;51(2):259–67.

35. Kadriu B, Gold PW, Luckenbaugh DA, Lener MS, Ballard ED, Niciu MJ, Henter ID, Park LT, De Sousa RT, Yuan P, Machado-Vieira R, Zarate CA. Acute ketamine administration corrects abnormal inflammatory bone markers in major depressive disorder. Mol Psychiatry. 2018;23(7)):1626–31.
36. Wang B, Jin H, Zhu M, Li J, Zhao L, Zhang Y, Tang D, Xiao G, Xing L, Boyce BF, Chen D. Chondrocyte beta-catenin signaling regulates postnatal bone remodeling through modulation of osteoclast formation in a murine model. ARTHRITIS RHEUMATOL. 2014;66(1):107–20.
37. Appelman-Dijkstra NM, Papapoulos SE. Clinical advantages and disadvantages of anabolic bone therapies targeting the WNT pathway. NAT REV ENDOCRINOL. 2018;14(10):605–23.
38. Sato A, Shimizu M, Goto T, Masuno H, Kagechika H, Tanaka N, Shibuya H. WNK regulates Wnt signalling and beta-Catenin levels by interfering with the interaction between beta-Catenin and GID. Commun Biol. 2020;3(1):666.
39. Shen YS, Chen XJ, Wuri SN, Yang F, Pang FX, Xu LL, He W, Wei QS. Polydatin improves osteogenic differentiation of human bone mesenchymal stem cells by stimulating TAZ expression via BMP2-Wnt/beta-catenin signaling pathway. STEM CELL RES THER. 2020;11(1):204.
40. Jiang T, Xia C, Chen X, Hu Y, Wang Y, Wu J, Chen S, Gao Y. Melatonin promotes the BMP9-induced osteogenic differentiation of mesenchymal stem cells by activating the AMPK/beta-catenin signalling pathway. STEM CELL RES THER. 2019;10(1):408.
41. Albers J, Keller J, Baranowsky A, Beil FT, Catala-Lehnen P, Schulze J, Amling M, Schinke T. Canonical Wnt signaling inhibits osteoclastogenesis independent of osteoprotegerin. J CELL BIOL. 2013;200(4):537–49.
42. Glass DN, Bialek P, Ahn JD, Starbuck M, Patel MS, Clevers H, Taketo MM, Long F, McMahon AP, Lang RA, Karsenty G. Canonical Wnt signaling in differentiated osteoblasts controls osteoclast differentiation. DEV CELL. 2005;8(5):751–64.
43. Fan J, Lee CS, Kim S, Zhang X, Pi-Anfruns J, Guo M, Chen C, Rahnama M, Li J, Wu BM, Aghaloo TL, Lee M. Trb3 controls mesenchymal stem cell lineage fate and enhances bone regeneration by scaffold-mediated local gene delivery. BIOMATERIALS. 2021;264:120445.
44. Joeng KS, Lee YC, Lim J, Chen Y, Jiang MM, Munivez E, Ambrose C, Lee BH. Osteocyte-specific WNT1 regulates osteoblast function during bone homeostasis. J CLIN INVEST. 2017;127(7):2678–88.
45. Sato MM, Nakashima A, Nashimoto M, Yawaka Y, Tamura M. Bone morphogenetic protein-2 enhances Wnt/beta-catenin signaling-induced osteoprotegerin expression. GENES CELLS. 2009;14(2):141–53.

Figures

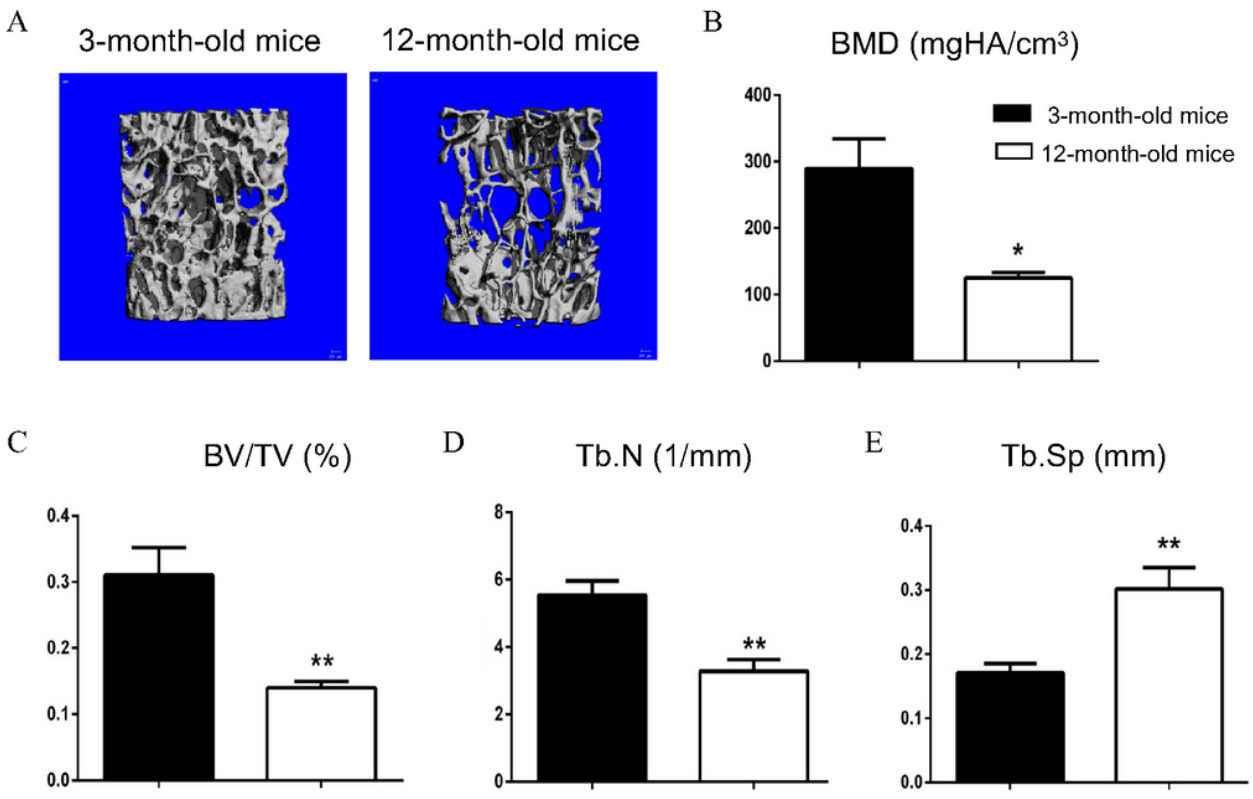

Figure 1

Bone mass was significant reduced in twelve-month-old mice. Three-month-old and twelve-month-old C57BL/6 mice were used to evaluate bone mass. (A) The μCT 3D image analysis of the forth lumbar vertebrae (L4) demonstrated a apparent bone loss in twelve-month-old mice compared with three-month-old mice. The quantitative analysis showed that bone volume (BV) and bone mineral density (BMD) were significantly decreased in twelve-month-old mice compared with three-month-old mice (B and C, n=6).

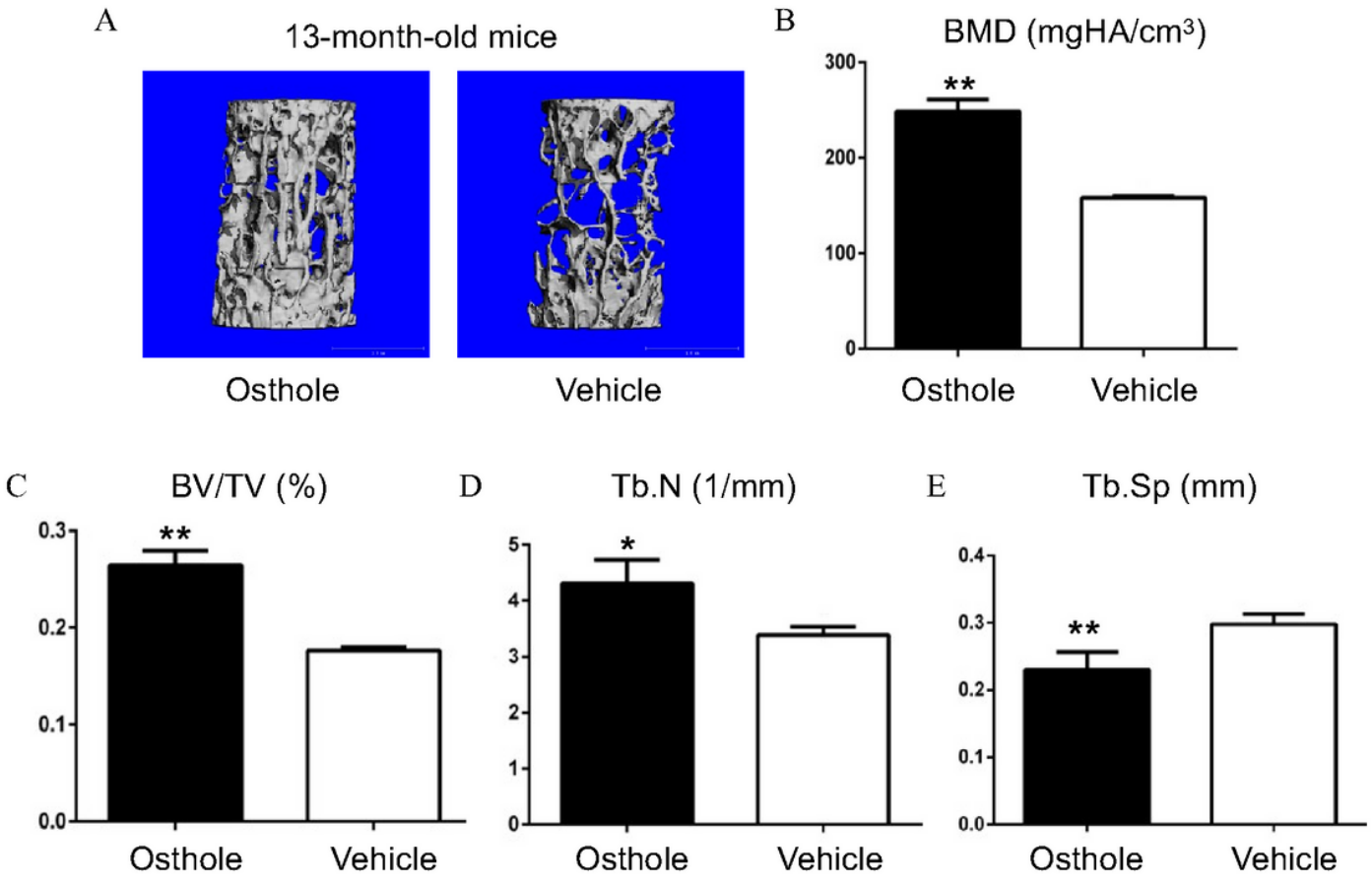

Figure 2

Osthole significantly increased bone mass of aged mice. Twelve-month-old C57BL/6J mice were treated with Osthole (5 mg/kg/day) or vehicle (corn oil) by intraperitoneal injection once a day for 4 weeks. Then, mice were sacrificed and the lumbar vertebrae were harvested for evaluation. (A) The μCT 3D image analysis of L4 samples showed that Osthole significantly increased bone mass in aged mice . (B and C) An apparent increase in bone volume (BV) and bone mineral density (BMD) was observed in aged mice after treated with Osthole by the quantitative analysis (n=6). (D and E) And osthole was found to significantly increase Tb.N($P<0.05$) and decrease Tb.Sp($P<0.05$) .*$P<0.05$, unpaired Student's t-test (Osthole versus vehicle).

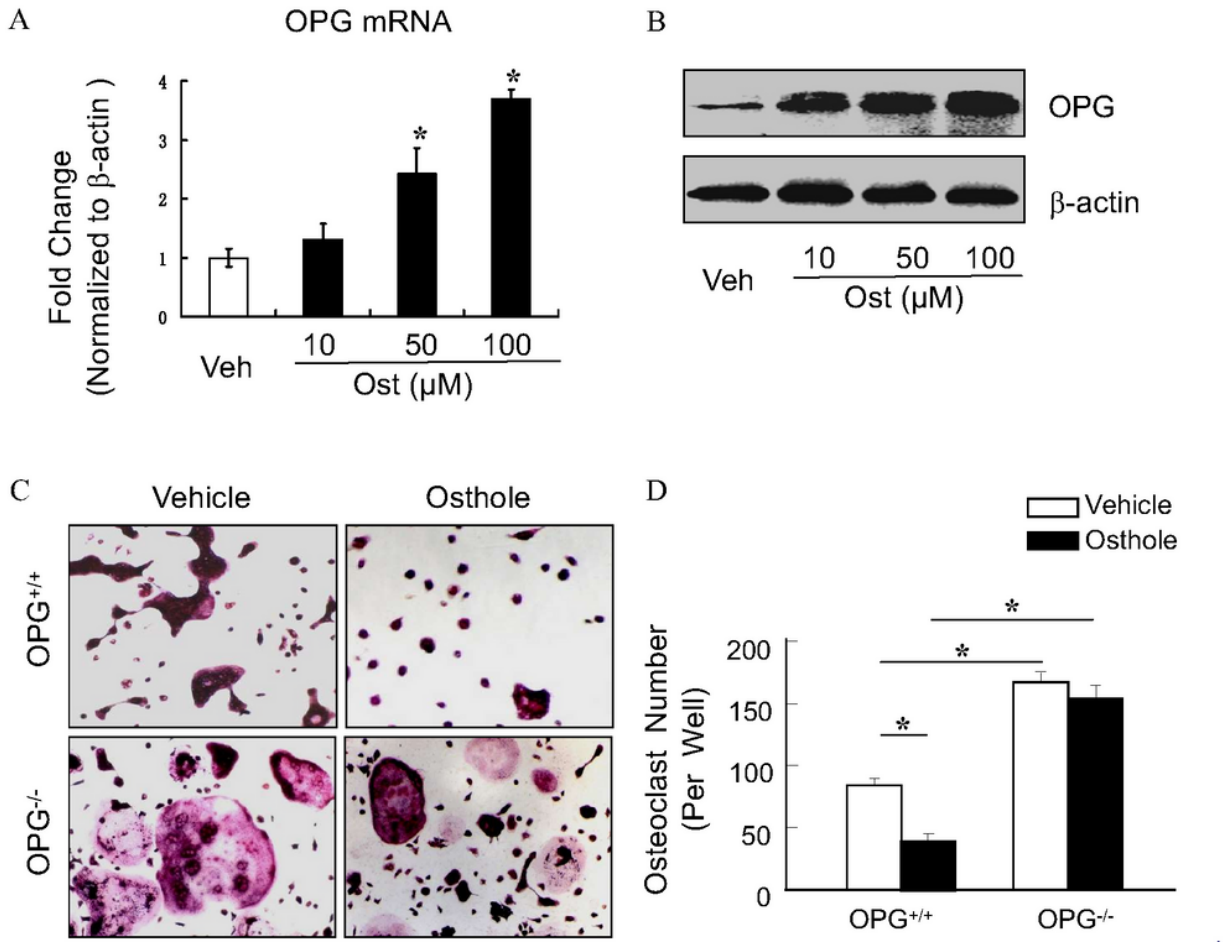

Figure 3

(A) Osthole inhibits osteoclast formation in aged mice. sections of L5 samples were performed the TRAP staining and found that Osthole decreased the number of osteoclast in aged mice. (B and C) The quantitative analysis demonstrated that the number of TRAP-positive multinucleated osteoclasts and the percentage of osteoclast surface were significantly decreased in aged mice after treated with Osthole (n=4). *P<0.05, unpaired Student's t-test (Osthole versus vehicle).

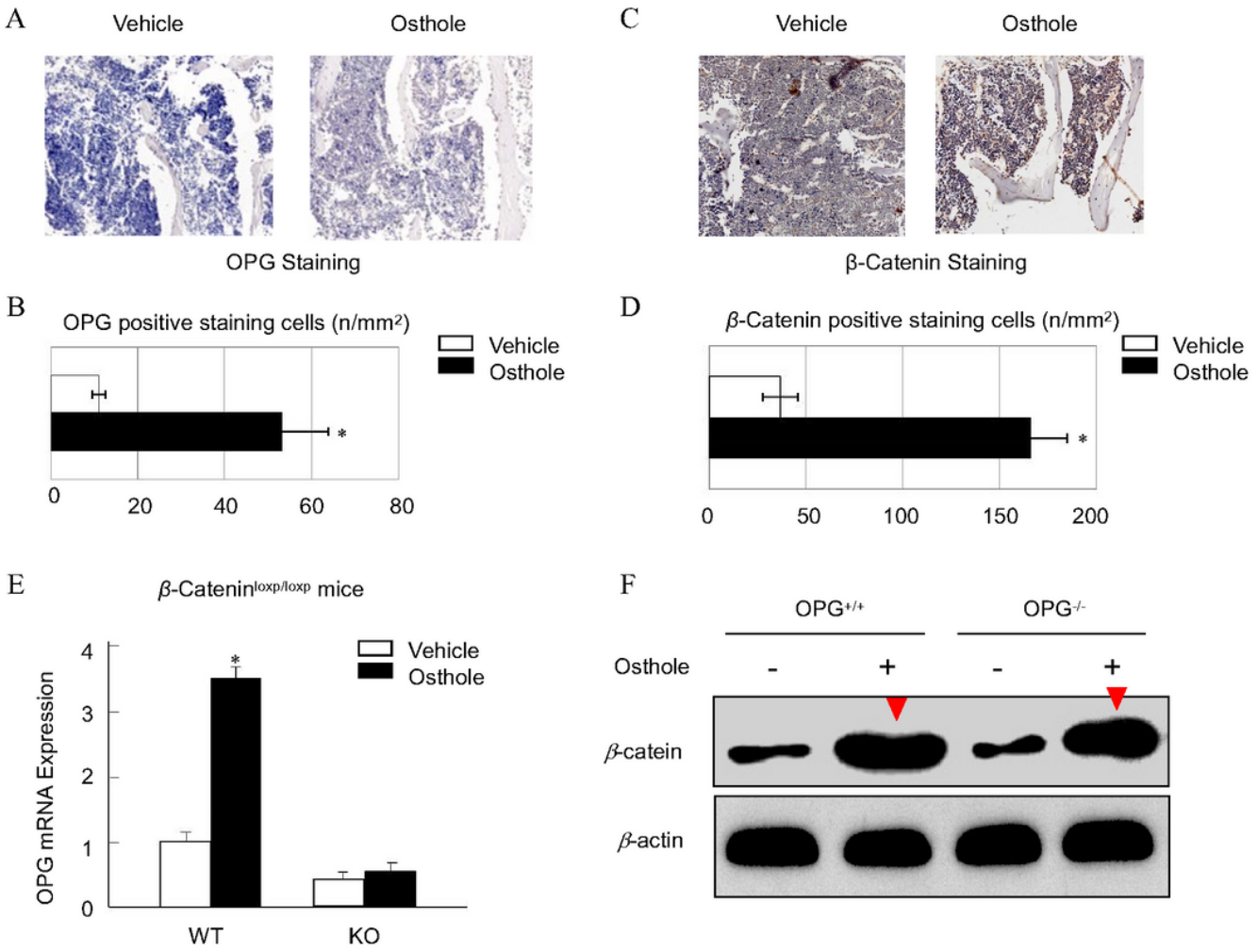

Figure 4

Osthole inhibits osteoclastogenesis in a dose-dependent and OPG-dependent manner. (A) BMSCs were cultured and treated with variation doses of Osthole (10-100 μM) or vehicle (DMSO)for 2 days, then OPG expression were detected using real-time PCR assay. All assays were performed in triplicate and repeated 3 times. Data were expressed as mean ± S.D. *P<0.05, unpaired Student's t-test (Osthole versus vehicle). (B) The protein expression of OPG was detected using Western-blot assay. A and B showed that Osthole significantly increased the mRNA and protein level of OPG expression in a dose-dependent manner, with the maximum effect at the dose of 100 μM. (C) BMCs were isolated from 3-month-old OPG-/- mice and its littermates of OPG+/+ mice, cultured with M-CSF (44 ng/ml) and RANKL (100 ng/ml), plus Osthole (100 μM) or vehicle for 7 days, then TRAP staining were performed. All assays were performed in triplicate and repeated 3 times. One representative view from each condition is shown. (D) Quantification of osteoclast number for Osthole in A. The number of multinucleated TRAP-positive cells (>3 nuclei) per representative view area at 40x magnification was obtained. Bars show averages of three replicates and data were expressed as mean ± S.D. *P<0.05, unpaired Student's t-test. C and D showed that Osthole inhibited the formation of osteoclasts in an OPG-dependent manner.

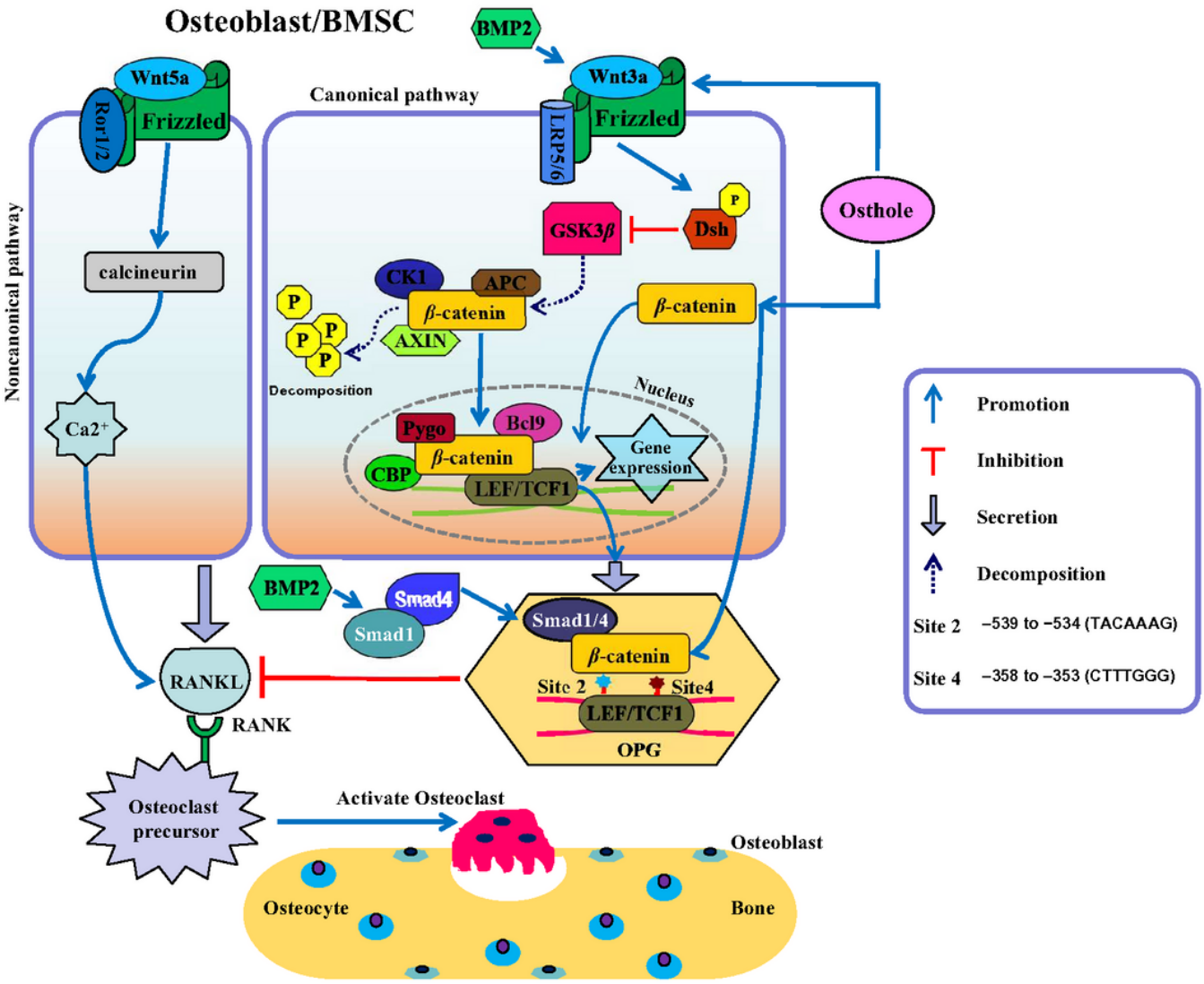

Figure 5

Osthole promotes the expression of OPG through activation of β-catenin signaling. (A) Twelve-month-old C57BL/6 mice were treated with osthole (5 mg/kg/day) or vehicle (corn oil) by intraperitoneal injection once a day. Mice were killed after 4 weeks, sections of the fifth lumbar vertebrae were prepared, OPG immunostaining was performed. Osthole increased the OPG protein level in aged mice. (B) β-catenin immunostaining was performed in L5 sections of Twelve-month-old C57BL/6 mice. Osthole increased the β-catenin protein level in aged mice. (C) BMSCs were isolated from 3-month-old β-Cateninfx/fx mice, infected with Ad-Cre or Ad-GFP, and treated with or without Osthole at the dose of 100uM. After 2 days, the total mRNA was collected and the expression of OPG was detected using real-time PCR assay. All assays were performed in triplicate and repeated 3 times. Data were expressed as mean ± S.D. *P<0.05, unpaired Student's t-test (Osthole versus vehicle). The deletion of β-Catenin by Ad-Cre infection significantly inhibited Osthole-induced expression of OPG. (D) BMSCs were isolated from 3-month-old OPG-/- mice and its littermates of OPG+/+ mice, treated with Osthole (100 μM) or vehicle for 2 days, the

total protein was collected and the expression of β-Catenin was detected using western-blot assay. The deletion of OPG didn't affect Osthole-induced expression of β-Catenin protein.

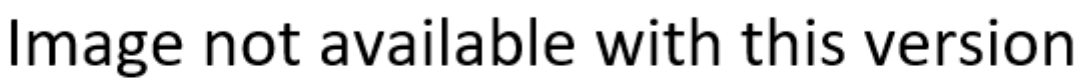

Figure 6

Schematic diagram of the mechanism through which Ostholeinhibits osteoclast formation and bone resorption.

Supplementary Files

This is a list of supplementary files associated with this preprint. Click to download.

- figures1.pdf